Transition State Analogue L-Leucinephosphonic Acid Bound to Bovine Lens Leucine Aminopeptidase: X-ray Structure at 1.65 Å Resolution in a New Crystal Form[†,‡]

Norbert Sträter and William N. Lipscomb*

Gibbs Chemical Laboratory, Harvard University, Cambridge, Massachusetts 02138

Received April 25, 1995; Revised Manuscript Received May 17, 1995[⊗]

ABSTRACT: The three-dimensional structure of bovine lens leucine aminopeptidase (blLAP) complexed with L-Leucinephosphonic acid (LeuP) has been determined by molecular replacement using the structure of native blLAP as a starting model. Cocrystallization of the enzyme with the inhibitor yielded a new crystal form of space group $P321$ which has cell dimensions $a = 130.4$ Å and $c = 125.4$ Å. Refinement of the model against data from 7.0 to 1.65 Å resolution resulted in a final structure with a crystallographic residual of 0.160 ($R_{free} = 0.191$). The N-terminal amino group of LeuP is coordinated to Zn-489, one phosphoryl oxygen atom bridges both metal ions, and another phosphoryl oxygen atom is coordinated to Zn-488. The side chain of Arg-336 interacts with the inhibitor via three water molecules. LeuP resembles the presumed tetrahedral *gem*-diolate transition state after direct attack of a water or hydroxide ion nucleophile on the scissile peptide bond. On the basis of the LeuP binding mode and the previous structural and biochemical data, three plausible reaction pathways are evaluated. The two-metal ion mechanisms discussed herein share as common features a metal-bound hydroxide ion nucleophile and polarization of the carbonyl group by the zinc ions. Possible catalytic roles of Arg-336 and Lys-262 in the direct or indirect (through H_2O) protonation of the leaving group, in the stabilization of a zinc-bound OH^- nucleophile and in the stabilization of the negatively charged intermediate, are discussed. A site 3 metal ion approximately 12 Å away from the active site 2 zinc ion probably serves a structural role.

Bovine lens leucine aminopeptidase (blLAP)[1] is a hexameric enzyme of molecular weight 324 kDa (Melbye & Carpenter, 1971; Carpenter & Harrington, 1972). The three-dimensional structures of the native enzyme and its complex with the natural inhibitors bestatin and amastatin have been determined previously (Burley et al., 1990, 1991, 1992; Kim & Lipscomb, 1993a,b, 1994). In our continuing effort to elucidate the enzyme mechanism by structural characterization of complexes with reaction coordinate analogues, we now report the X-ray structure of L-leucinephosphonic acid (LeuP) bound to blLAP. The high-resolution structure in a new crystal form allows for a detailed analysis of the possible interactions between the enzyme and the presumed tetrahedral *gem*-diolate intermediate or transition state and for an independent re-evaluation of the results achieved so far.

Leucine aminopeptidase [LAP, α-aminoacyl-peptide hydrolase (cytosol), EC 3.4.11.1] is an exopeptidase that catalyzes the removal of amino acids from the *N*-terminus of a peptide [for reviews, see Smith and Hill (1960), Delange and Smith (1971), Hanson and Frohne (1976), Kim and Lipscomb (1994)]. Aminopeptidases are ubiquitous in nature and are of critical biological and medical importance because of their key role in protein modification and degradation and in metabolism of biologically active peptides (Taylor, 1993a,b). Altered aminopeptidase activity has been associated with several pathological disorders such as cancer (Umezawa, 1980) and possibly eye lens cataracts (Taylor et al., 1982).

LAP has been intensively characterized by biochemical studies of metal ion function and activation and of inhibition by various noncovalently acting ligands. Each of the six identical 54 kDa subunits of blLAP contains two zinc ions (Carpenter & Vahl, 1973) that are essential for catalytic activity and that display different exchange kinetics. The two metal ions are 2.9 Å apart in the native enzyme (Burley et al., 1990). The readily exchangeable site 1 can stoichiometrically bind Zn^{2+}, Mn^{2+}, Mg^{2+}, or Co^{2+} (Carpenter & Vahl, 1973; Thompson & Carpenter, 1976a,b; Allen et al., 1983) and has been identified as Zn-488 in the X-ray structure by the structure determination of the $Zn^{2+}-Mg^{2+}$ metallohybrid enzyme (Kim & Lipscomb, 1993). The zinc ion in the tight binding site 2 can be exchanged against Co^{2+} only when both binding sites are unoccupied (Thompson & Carpenter, 1976b; Allen et al., 1983). In contrast to some earlier results, it is now apparent that metal substitution in both binding sites significantly affects both K_m and k_{cat} (Allen et al., 1983). Thus, both metals participate in substrate binding and activation including a possible role in the activation of the nucleophile.

Bestatin and amastatin are among the strongest known inhibitors of LAP (Umezawa et al., 1976; Aoyagi et al., 1978; Taylor et al., 1993; Rich et al., 1984). Due to the hydroxyl group at the P_1 residue of these inhibitors, both compounds

[†] This work was supported by NIH Grant GM 06920 (W.N.L.). N.S. thanks the Deutsche Forschungsgemeinschaft for financial support.

[‡]The coordinates have been deposited in the Brookhaven Protein Data Bank, Brookhaven National Laboratories, Upton, Long Island, NY 11973, under file name 1LCP.

* Author to whom correspondence should be addressed.

[⊗] Abstract published in *Advance ACS Abstracts,* July 1, 1995.

[1] Abbreviations: LAP, leucine aminopeptidase; blLAP, bovine lens leucine aminopeptidase; pkLAP, porcine kidney leucine aminopeptidase; LeuP, L-leucinephosphonic acid; LV, L-leucyl-L-valine; LVTS, putative *gem*-diolate transition state for the proteolysis of L-leucyl-L-valine; MPD, 2-methyl-2,4-pentanediol; rms, root mean square; *B*-factor, temperature factor; F_o and F_c, observed and calculated structure factors.

0006-2960/95/0434-9200$09.00/0

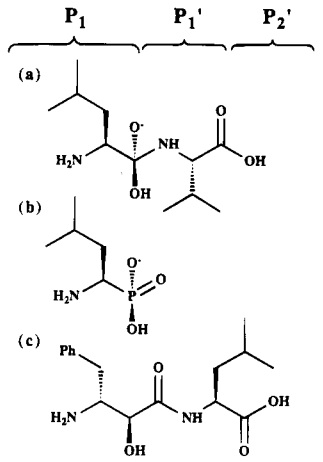

FIGURE 1: Transition state and inhibitors of blLAP catalysis: (a) *gem*-diolate transition state LVTS of substrate L-leucyl-L-valine (LV), (b) L-Leucinephosphonic acid, and (c) bestatin. The peptide residues have been labeled according to the convention of Schechter and Berger (1967).

are thought to mimic the tetrahedral transition state (Figure 1). However, the fact that both inhibitors bear an additional carbonyl group compared to a natural peptide substrate complicates the interpretation of the structural results. A reduced bestatin isostere, in which this carbonyl group was replaced with a methylene group, displayed a 50 000-fold reduced binding affinity toward pkLAP (Harbeson & Rich, 1988). This result indicates the importance of the P_1 carbonyl group for the binding of these inhibitors. The X-ray structures of the blLAP−bestatin and blLAP−amastatin complexes showed that the carbonyl oxygen interacts with the side chain of Lys-262. Both inhibitors were found to be bound in the same N-to-C-terminus orientation and with the amino group coordinated to Zn-489. The P_1 hydroxyl group coordinates to both metal ions. The tight binding of bestatin and amastatin is also remarkable considering the fact that the P_1 side chains of these inhibitors are configured like a D-amino acid. Substrates with an N-terminal amino acid in the D-configuration, like D-leucylglycine, D-leucyl-L-tyrosine, or D-leucineamide, are not hydrolyzed by LAP (Smith & Hill, 1960; Delange & Smith, 1971).

A number of different reaction coordinate analogue inhibitors have been reported to bind to LAP. Among these are phosphorus amino acid analogues, which mimic the tetrahedral *gem*-diolate transition state of an associative mechanism for peptide hydrolysis (Figure 1) (Giannousis & Bartlett, 1987). Phosphonate and phosphoamidate inhibitors are excellent inhibitors of the zinc metallopeptidases carboxypeptidase A or thermolysin and have also been used to study the mechanisms of these enzymes (Christianson & Lipscomb, 1988; Kim & Lipscomb, 1991; Matthews, 1988). It is noteworthy that one of the strongest known enzyme inhibitor interactions has been determined (Kaplan & Bartlett, 1991) and structurally characterized (Kim & Lipscomb, 1991) between such a phosphonate tripeptide analogue and carboxypeptidase A (K_i = 11 fM). Compared to these tight interactions, phosphonic acid analogues are significantly less potent inhibitors of LAP. L-Leucinephosphonic acid and L-phenylalaninephosphonic acid, which are the strongest known binding analogues with respect to pkLAP, have K_i-values of 0.23 and 0.42 μM, respectively. The P−C bond of these inhibitors is 0.3 Å longer than the $(sp^3)C-(sp^3)C$ bond in the putative intermediate, and a P−O bond is 0.1 Å longer than a C−O bond. Moreover, the phosphorus amino acid analogues contain one sp^2 hybridized oxygen at the tetrahedral phosphorus, whereas in the *gem*-diolate transition state all atoms next to the former carbonyl carbon atom are sp^3 hybridized (Figure 1; Kim & Lipscomb, 1994). Although the binding of these compounds to blLAP is significantly less tight than that of other phosphorus amino acid and peptide analogues to mononuclear zinc enzymes, it should be kept in mind that their inhibition constant is still ca. 2−4 magnitudes smaller than the binding constant of a typical substrate (Fittkau et al., 1974).

Besides blLAP, two other aminopeptidases employing a two-metal ion center in catalysis have been structurally characterized, *Aeromonas proteolytica* aminopeptidase (AAP) with a dinuclear zinc site (Chevrier et al., 1994) and the cobalt enzyme methionine aminopeptidase M (MAP) (Roderick & Matthews, 1993). In AAP the two zinc ions are 3.5 Å apart and bridged by an aspartate side chain and a water ligand. Both zinc ions are further coordinated by an aspartate or glutamate carboxylate group and by a histidine. AAP displays structural homology to the C-terminal domain of LAP, although neither are the active site ligands in equivalent positions nor are the active sites similar. In MAP the geometry of the coordination sphere of both cobalt ions is approximately octahedral with two ligand positions not occupied or occupied by the second cobalt ion at a distance of 2.9 Å. The active site structures of all three structurally characterized aminopeptidases each containing a dimetal center are significantly different and obviously constitute different types of proteolytic enzymes.

The high-resolution crystal structure of blLAP complexed with L-leucinephosphonic acid allows for a detailed analysis of the enzyme−inhibitor interactions. On the basis of this structure, the implications on the reaction mechanism and especially on the roles of the dinuclear zinc center and the enzymic active site residues in catalysis are discussed. The aim of this study also includes the re-evaluation of the conclusions drawn from the structures of the blLAP − bestatin and blLAP−amastatin complexes, which, as already pointed out, despite their tight binding do not constitute perfect reaction coordinate analogues. The role of the active site Arg-336, which on the basis of the previous structures has been described as being present in alternate conformations and directly interacting with the substrate, needs some reconsideration.

MATERIALS AND METHODS

blLAP was isolated from bovine calf eye lenses according to the method of Carpenter (Allen et al., 1983). L-Leucinephosphonic acid was a gift from P. Bartlett (Giannousis & Bartlett, 1987). The enzyme was cocrystallized with the inhibitor by equilibrating a hanging drop (20 μL) of 7 mg/ml blLAP, 10 mM L-leucinephosphonic acid, 50 μM $ZnSO_4$, 200 mM NaCl, and 50 mM Tris·HCl, pH 7.8, against a solution of 1:1 (v:v) 50 mM Tris·HCl/50 μM $ZnSO_4$:2-methyl-2,4-pentanediol (MPD) (Jurnak et al., 1977). Within 2 weeks crystals of two different morphologies appeared, hexagonal, rodlike crystals and more compact crystals. One of the latter crystals of dimensions 0.4 × 0.4 × 0.4 mm was directly mounted from the drop for data collection.

X-ray diffraction data were collected at −150 °C on a Siemens X-1000 multiwire area detector. Monochromated

Table 1: Details of Data Collection and Refinement

Data Set Statistics	
space group	$P321$
cell axes (Å)	$a = 130.4$, $c = 125.4$
max resolution (Å)	1.65
no. of crystals	1
temperature (°C)	−150
reflections measured	766 198
unique	144 211
completeness (%)[a]	97.7 (90.7)
$> 2\sigma F$ (%)[a]	84.2 (55.2)
R_{sym}[a]	0.074 (0.26)
V_m (Å^3/Da)	2.8
Refinement Statistics	
resolution range (Å)	7.0−1.65
R/R_{free}	0.160/0.191
protein atoms ($Z > 1$)	7404
water molecules	968
ligand atoms	68
rmsd bond length (Å)	0.010
bond angles (deg)	1.7
dihedral angles (deg)	21.8
improper twist angles (deg)	1.37
average B protein (Å^2)	12.7
waters (Å^2)	23.3
LeuP (Å^2)	11.2
MPD (Å^2)	18.5
Ramachandran plot outliers	0

[a]The values in parentheses are for the highest resolution shell (1.7−1.65 Å).

Cu Kα radiation was produced by an Elliot GX3 rotating anode generator with a 200 μm focus cup operating at 35 kV and 40 mA and a Supper double-mirror system of two nickel-coated glass mirrors. A Siemens LT-2 low-temperature apparatus was used to maintain the temperature. The crystal was mounted in a hair loop free standing film of the MPD crystallization solution. Details of data collection and data reduction are summarized in Table 1. The program XDS was used for data reduction (Kabsch, 1988). Although the unit cell dimensions were similar to those of the native crystals in space group $P6_322$ ($a = b = 132$ Å and $c = 122$ Å) and both crystals belong to the trigonal/hexagonal Bravais lattice, it was immediately apparent that the weighted reciprocal lattice of the blLAP−LeuP data set has only $\bar{3}$m1 symmetry. No systematic absences were apparent for the 000l reflections, so that the space group could be unambigously determined as $P321$. The asymmetric unit of blLAP in space groups $P6_322$ and $P321$ contains one and two subunits of the hexamer, respectively.

The coordinates of the native structure of blLAP were used for structure solution by molecular replacement. The rotation and translation functions were solved with the program AMORE (Navaza, 1994) using one monomer of the hexamer as the search model. The top two peaks of the rotation function were found to be the correct solutions. They had peak heights of 4.8- and $3.8\sigma_{rms}$. The top peaks of the translation function were also found to be correct and yielded R-factors of 0.517 and 0.518 for each monomer after rotation and translation. Placement of both monomers into the asymmetric unit resulted in an R-factor of 0.441. Crystallographic refinement was performed using XPLOR (Brünger, 1992a). Ten percent of the measured reflections was set aside throughout all refinement steps and used to calculate the free R-factor (Brünger, 1992b). No constraints or restraints relating to the noncrystallographic symmetry relation between the two subunits in the asymmetric unit were used at any step of the refinement. The position of the blLAP−LeuP complex in the unit cell was improved by rigid body refinement subject to the assumption that each monomer within the asymmetric unit was rigid but independent of the other. The initial model was first refined by several rounds of simulated annealing at 3000 K (Brünger et al., 1990) to remove model bias; subsequent refinement was performed using alternating rounds of manual rebuilding and positional minimization. All model building was done with the program O (Jones & Kjeldgaard, 1994). Solvent molecules were included gradually from $F_o - F_c$ electron density maps, if the peak height was stronger than $4\sigma_{rms}$ and the position was near (2.5−3.5 Å) a suitable hydrogen-bonding donor or acceptor, and were kept in the refinement if the B-value did not exceed 40 Å^2. Inclusion of additional water molecules from $F_o - F_c$ maps was stopped when the R_{free} did not decrease in the subsequent minimization run. The model for L-leucinephosphonic acid was included into the refinement when most of the protein was already well refined and the difference electron density ($F_o - F_c$) for the inhibitor was well defined. At this stage the R-factor was 0.217. The refinement parameters for LeuP and MPD were determined using QUANTA (Molecular Simulations Inc., 1994). The zinc−ligand distances were not restrained in the refinement, and the van der Waals radii of the zinc ions were set to zero. This procedure guarantees that the refined metal−ligand distances are not subject to any bias. The matrices for a superposition of different blLAP models or subunits were calculated by a least-squares distance minimization algorithm implemented inside O using the C_α atoms as the guide coordinates, even if the rms difference had been analyzed for other atom types. Details of the refinement are listed in Table 1. Figures 3−6 and 10 were prepared using MOLSCRIPT (Kraulis, 1991) and Figure 2 was calculated using O (Jones & Kjeldgaard, 1994).

RESULTS

The final refined structure of the blLAP−LeuP complex contains 968 amino acid residues (residues 1−484 of two monomers), 6 zinc ions, 968 water molecules, 6 MPD molecules (2-methyl-2,4-pentanediol), and 2 LeuP molecules in the asymmetric unit; 28 side chains were found and refined in alternate conformations. The model shows good stereochemistry (Table 1), and the Luzzati plot (Luzzati, 1952) indicates a coordinate error of 0.15−0.20 Å. Residues 12−14, which could not be located in previous blLAP structures, were now included into the model. The electron density of this region allowed for an unambigous placement of the main chain and of the side chain of Glu-12. Lys-13 and Glu-14 have very weak side chain density in both monomers of the asymmetric unit but were included since the positions of the C_β atoms were obvious. As in the previously reported structures of blLAP there was no interpretable electron density for the C-terminal residues 485−487, which seem to be intrinsically disordered.

Six MPD molecules from the crystallization buffer are bound to the surface of the protein. The electron density was well defined for the MPDs and could not be interpreted as bound LeuP. Assignment of the two hydroxyl oxygens could be made by an analysis of the hydrogen-bonding interactions. All bound MPD molecules are more than 25 Å away from the active site and probably do not have any effect on the enzyme or the active site structure.

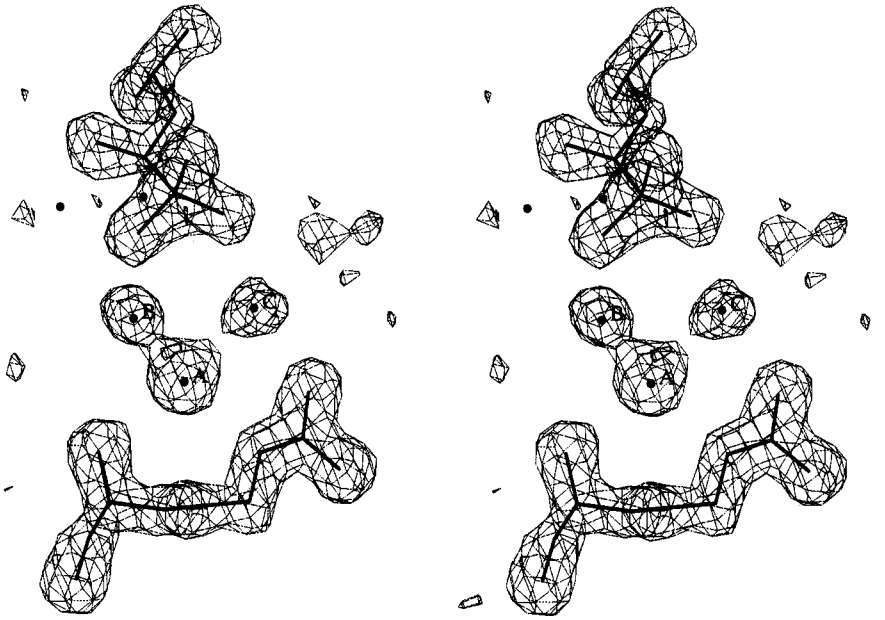

FIGURE 2: Stereoview of the $F_o - F_c$ electron density map of Arg-336 (bottom) and the active site water molecules A−C and LeuP (top). These residues have been omitted from the refined model in the calculation of the density. Also shown are the two zinc ions. The contour level of the map is $2.5\sigma_{rms}$. At a higher contour level the water molecules A and B show separated density. The model and density shown here and in all other figures refer to subunit I of the asymmetric unit. There are no significant differences between the active site structures of subunits I and II.

Overall Structure. blLAP is physiologically active as a hexamer of 32 symmetry. The packing of the hexamer in space groups $P6_322$ and $P321$ is very similar. In the space group $P6_322$ the symmetry of the hexamer is completely incorporated into the space group symmetry. In the blLAP−LeuP cocrystal structure in the space group $P321$ only the 3-fold axis of the hexamer is part of the space group symmetry. The 2-fold axes relating the two trimers of the hexamer are noncrystallographic symmetry axes. The difference between these space groups can be described as a rotation of the whole hexamer by 1.5° around the 3-fold axis and a translation by 0.5 Å along this axis. Superposition of the two subunits within the asymmetric unit yielded rms deviations of 0.22 and 0.72 Å for the main chain and side chain atoms, respectively. The small rms deviations demonstrate that both subunits are very similar and that the crystal packing interactions have no significant influence on the overall structure. The enzyme structure of the blLAP−LeuP complex is also very similar to the structure of the native enzyme and the blLAP−bestatin and blLAP−amastatin complexes. The superposition of the structure of native blLAP onto the structure of the blLAP−LeuP complex yielded an rms deviation of 0.9 Å for the main chain coordinates, if the whole hexamer was used for the superposition. If only one subunit was superimposed, a smaller rms deviation of 0.36 Å was calculated. Besides the movement of the whole hexamer, the structures in both space groups obviously differ also by a small relative movement of the two subunits that are related by the 2-fold symmetry axis of the hexamer. A detailed analysis of the packing interactions in both space groups showed that about one-half of the interhexamer interactions in the crystal lattice in space group $P321$ is different from those in the structure in $P6_322$. Although the crystallization in the new space group resulted in many different packing interactions, the overall enzyme structure is not significantly affected by these interactions. It is also apparent that the enzyme structure shows no structural changes induced by the inhibitor binding, in agreement with the inhibitor structures previously elucidated. Since the active site structure is similar to that of the previous structures, and the active site in the center of the hexamer is also unlikely to influence the crystal packing, the crystallization in a new space group is obviously not caused by the binding of the inhibitor to the active site. Because there were also no additional binding sites found for LeuP, it seems likely that the new crystal form was induced by a change of the properties of the solution from which the crystals were obtained.

LeuP Binding Mode. One molecule of LeuP binds to the active site of blLAP (Figures 2 −4, Table 2). The binding mode is similar to that of bestatin and amastatin but also shows an additional interaction of oxygen O2 with the dimetal center. As in the previous inhibitor complexes, the terminal amino nitrogen is coordinated to Zn-489, the tightly bound site 2 metal ion. One of the phosphoryl oxygens, O1, bridges both metal ions but is somewhat closer to Zn-489. A water molecule (B) is hydrogen bonded to O1 as well as to the backbone nitrogen of Gly-335 and the backbone carbonyl oxygen of Leu-360. The second phosphoryl oxygen, O2, is coordinated to Zn-488 and hydrogen bonded to Lys-262. The third phosphoryl oxygen, O3, interacts via a 3.2 Å (II:[2] 3.1 Å) hydrogen bond with the backbone carbonyl oxygen of Leu-360. Also, O3 is hydrogen bonded to two water molecules: water molecule D, which is also hydrogen bonded to the backbone nitrogen of Gly-362, and water molecule C, which is also hydrogen bonded to the guanidinium nitrogen $N_\eta 1$ of Arg-336 and the carbonyl oxygen of Leu-360 (see below).

Coordination Sphere of the Metal Ions. Both metal ions are coordinated by five ligands in the first coordination sphere ($d < 2.4$ Å), but each contains a sixth ligand in the second coordination sphere: the bridging O1 of LeuP coordinated to the site 1 zinc ion and the carboxylate oxygen

[2] The values in parentheses refer to subunit II, related by noncrystallographic symmetry, in the asymmetric unit.

Table 2: Selected blLAP−LeuP Distances (Å)[a]

inhibitor atom	enzyme atom	subunit I	subunit II
terminal amino N	Zn-489 (site 2)	2.28	2.24
	Asp-273 $O_{\delta}2$	2.89	2.85
	Asp-273 $O_{\delta}1$	3.16	3.08
	Asp-255 $O_{\delta}1$	3.15	3.15
	Lys-250 N_{ζ}	3.49	3.51
phosphoryl O1	Zn-488 (site 1)	2.49	2.53
	Zn-489 (site 2)	2.26	2.22
	Asp-332 carbonyl O	3.10	3.09
	Lys-250 N_{ζ}	3.28	3.23
	Glu-334 $O_{\epsilon}1$	3.01	3.00
	Glu-334 $O_{\epsilon}2$	3.14	3.08
	Asp-255 $O_{\delta}1$	3.35	3.38
	water O_B	2.68	2.63
phosphoryl O2	Asp-255 $O_{\delta}1$	3.08	3.03
	Lys-262 N_{ζ}	2.68	2.74
	Zn-488 (site 1)	2.11	2.07
	Zn-489 (site 2)	3.83	3.75
	Asp-332 $O_{\delta}1$	3.49	3.58
	Asp-332 $O_{\delta}2$	2.87	2.91
	Asp-332 carbonyl O	3.02	3.01
phosphoryl O3	Leu-360 carbonyl O	3.24	3.10
	water O_C	2.77	2.61
	water O_D	2.60	2.74

[a]Note: the number of digits given does not necessarily reflect the number of significant digits within the error limit of the value.

$O_{\delta}1$ of Asp-255 near the site 2 zinc ion (Figure 3, Table 3). With these six ligands the coordination geometry around the two metal ions matches two distorted octahedra that are connected by the asymmetrically bridging phosphoryl oxygen O1 and by $O_{\delta}1$ of Asp-255. The average deviations from 90° of the angles around the zinc ions are 7.6° (II: 7.9°) for Zn-488 and 7.4° (II: 6.9°) for Zn-489. The largest deviations from a 90° angle are shown by angles O1, LeuP/Zn-488/O2, LeuP (~66°) and $O_{\epsilon}2$, Glu-334/Zn-488/$O_{\delta}2$, Asp-332 (~116°) on the opposite side. Whereas the carboxylate oxygen $O_{\delta}1$ of Asp-255 is coordinated to Zn-488 by its *syn* orbital, Zn-489 is neither in the direction of the *anti* orbital of $O_{\delta}1$ nor within the plane of the carboxylate group. Thus, according to the preferred metal−carboxylate group interactions (Chakrabarti, 1990; Glusker, 1991), Asp-255 is only weakly interacting with Zn-489; this bridge is not a monodentate *syn,anti* carboxylate bridge. This weak interaction between $O_{\delta}1$ of Asp-255 and Zn-489 is also reflected by the long coordinating distance of 2.7 Å. The two metal ions have similar temperature factors of 10.7 Å^2 (II: 10.8 Å^2) in site 1 and 9.6 Å^2 (II: 9.8 Å^2) in site 2. The metal−metal distance is 3.4 Å. This distance is 3.1 and 3.3 Å in the blLAP−bestatin and blLAP−amastatin complexes, respectively.

Interactions Around Arg-336. The three water molecules interacting with Arg-336 and the LeuP oxygens O1 and O3 are shown in Figure 2 together with the observed electron density. In the previous crystal structure determinations of the native enzyme as well as of the inhibitor complexes, a similar V-shaped electron density was observed next to Arg-336 at the same position. This density was then interpreted as two different conformations of Arg-336 in the native enzyme as well as in the presence of bestatin or amastatin. It was suggested that the alternate conformation of Arg-336 might interact directly with the substrate and the transition state during catalysis. The current structure provides four indications that this V-shaped density results from three water molecules hydrogen bonded to Arg-336. First, the $F_o - F_c$ electron density map showed three separated peaks at the positions which now correspond to the three water molecules before these water molecules were added to the model. The water positions are in good hydrogen-bonding distances to protein side chain and main chain atoms and the phosphoryl oxygens (Figure 4, Tables 2 and 3). Two of these water positions (waters A and B) are very close together (2.3 Å, II: 2.1 Å) and may not be occupied simultaneously. A refinement of the occupancy of all water molecules using an average temperature factor of 15 Å^2 for the waters yielded occupancies of 1.1 (II: 0.8) and 1.3 (II: 0.8) for water molecules A and B, respectively. The average occupancy of the 100 strongest occupied water positions was 1.36. However, the crystallographic temperature factor of a water molecule can vary significantly. Moreover it is not possible to refine independently the *B*-value and the occupancy, even at 1.65 Å resolution. Thus, the occupancy refinement cannot provide an unambigous answer to the question, as to whether both water positions are occupied simultaneously. Second, the electron density maps show even at low contour levels no density between the V-shaped density island and the Arg-336 side chain or main chain atoms. Third, Arg-336 has strong and well-defined density, which does not indicate a partially occupied conformation. The average temperature factor for the Arg-336 side chain atoms is 8.8 Å^2 (II: 10.0 Å^2). A refinement of the occupancy of all arginine side chains resulted in an occupancy of 1.16 (II: 1.11) for Arg-336. The average occupancy of all arginine side chains was 0.98, the lowest value observed was 0.26 for the solvent-exposed Arg-425 side chain, and the highest value observed was 1.32 for Arg-470. In order to obtain these occupancies, the *B*-values of all protein atoms were reset to 10.0 Å^2 for the occupancy refinement. Fourth, the side chain of Arg-336 was also modeled and refined in the alternate conformation occupying the density of the three water molecules, A−C. The refinement resulted in a significantly higher average temperature factor of 24.7 Å^2 (II: 24.3 Å^2) for the side chain atoms of Arg-336.

Site 3 Metal-Binding Site. Besides the two active site zinc ions another metal ion was found in the crystal structure (Figure 5). Refinement as a water molecule gave an unusually low temperature factor, and the subsequent difference electron density map showed the strongest peak at this position. A zinc ion was then refined at this position because 50 μM $ZnSO_4$ was present in the crystallization buffer. The zinc ion has a reasonable temperature factor of 19.3 Å^2 (II: 18.6 Å^2). The metal ion is coordinated by the backbone carbonyl oxygen atoms of Leu-170 (distance 2.8 Å), Met-171 (2.8 Å), Thr-173 (2.7 Å), and Arg-271 (2.7 Å) and by a water ligand (2.7 Å). S_{δ} of Met-274 is 3.5 Å away from the metal ion. The coordination sphere around the site 3 metal has distorted trigonal bipyramidal geometry with the carbonyl oxygen of Met-171 and the water molecule in the axial positions. Whereas a 5-fold coordination is not unusual for a zinc ion, the relatively long metal−oxygen distances and the overall neutral charge of the coordination sphere are not typical for a zinc ion ligand sphere and seem to be more suitable for a monovalent ion like Na^+ or K^+. Sodium ions were present at a concentration of 200 mM in the crystallization medium, but the electron density peak appears to be too strong for a sodium ion. An occupancy refinement of H_2O, Na^+, K^+, and Zn^{2+} in this position yielded values of 2.8 (II: 2.9), 1.9 (II: 2.0), 1.2 (II: 1.2), and 0.7 (II: 0.7),

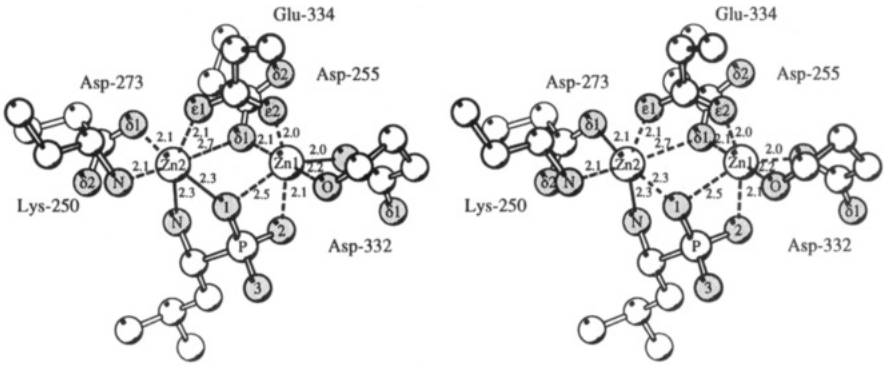

FIGURE 3: Coordination sphere of the dizinc center and binding mode of LeuP including the metal−ligand distances. Nitrogen and oxygen atoms are shown in gray. In addition, the nitrogen atoms are labeled "N" and the oxygen atoms by their atom type.

Table 3: Additional Interactions of the Active Site Water Molecules (Distances in Å)[a]

residue	residue	subunit I	subunit II
Gly-335 peptide N	water O_B	2.93	2.99
Arg-336 peptide N	water O_A	3.04	3.13
Arg-336 N_ϵ	water O_A	2.87	2.91
Arg-336 $N_\eta 1$	water O_C	2.84	2.99
Leu-360 carbonyl O	water O_C	3.21	3.28
Leu-360 carbonyl O	water O_B	3.15	3.20
water O_A	water O_B	2.28	2.13
water O_A	water O_C	2.85	2.64

[a]Note: the number of digits given does not necessarily reflect the number of significant digits within the error limit of the value.

respectively. A temperature factor of 10 Å^2 was used in the occupancy refinement, which is approximately the average *B*-factor of this region. It cannot be said with certainty which metal ion was bound at this position under the crystallization conditions and in the crystal structure. In the absence of any potassium ions in the solution besides trace amounts, it seems unlikely that a potassium ion is bound here. The binding site is most probably occupied by a zinc ion that has a higher *B*-value than the surrounding protein residues because the binding site is not perfect for zinc. Alternatively, the binding site may be occupied only partially. However, in the presence of other metal ions in the cell, this metal-binding site may selectively bind other ions, like K^+.

The site 3 metal ion is located at the carboxy end of the α-helix from residues 151 to 172. This helix connects the N- and the C-terminal domains [for a topology diagram, see Burley et al. (1992)]. Three of the four protein ligands to the metal ion are contributed by the loop after this helix. This metal ion is ~12 Å away from Zn-489 of the same monomer. The closest connection between the site 3 metal ion and the active site occurs between the carbonyl group of Arg-271, which is coordinated to the site 3 metal ion, and the side chain of Asp-273, which is coordinated to Zn-489 and hydrogen bonded to the amino group of the inhibitor. It seems likely that this metal ion serves a structural role, possibly stabilizing part of the interface between the N-terminal and the catalytic domain.

DISCUSSION

Inhibitor Binding Modes. The similarity between the binding mode of the natural inhibitors bestatin and amastatin and the LeuP binding mode demonstrates that the former inhibitors are, despite their imperfections, good transition state analogues and obviously do not bind in an un-natural way (Figure 6). The fact that bestatin contains an additional carbonyl group between the tetrahedral carbon atom and the peptide NH group is reflected in a different interaction pattern in this region. The phosphoryl oxygen O2 is directly coordinated to Zn-488, whereas the carbonyl oxygen of bestatin is not coordinated to the metal ion. Both oxygens are, however, hydrogen bonded to Lys-262.

Figure 7 shows an analysis of the hydrogen-bonding pattern in the active site region. The hydrogen positions could be assigned unambigously to the noncarbon atoms and are consistent with the water positions determined by the X-ray data. The analysis also allows for a proposal of the protonation mode and the electronic structure of the phosphoryl oxygen atoms. O1 is most likely the negatively charged sp^3 hybridized oxygen, since it accepts three coordinating or hydrogen bonds. O2 may then be the sp^2 hybridized oxygen consistent with two coordinating or hydrogen bonds. O3 may be protonated because it is in hydrogen-bonding distance to the carbonyl group of Leu-360.

Mechanism of Catalysis. Most of the studies on LAP catalysis made so far, including the X-ray structural determinations of blLAP, implicate that the scissile carbonyl group of the intact substrate is directly attacked by an active site water molecule. The reaction proceeds via a tetrahedral *gem*-diolate transition state or intermediate, which is not covalently bonded to the enzyme. In the structures of blLAP and its complexes with inhibitors, there are no nucleophilic amino acid residues in the active site which are in position for a direct nucleophilic attack on the scissile substrate carbonyl group.

Provided that the binding mode of LeuP to the active site of blLAP is similar to that of the *gem*-diolate intermediate, the positions of the phosphoryl oxygen atoms can be assigned to the following three atoms around the tetrahedral *gem*-diolate carbon atom: the former carbonyl oxygen O_c of the scissile peptide bond, which presumably bears a negative charge, the former attacking water or hydroxide ion nucleophile O_n, and the former peptide nitrogen atom. Thus, on the basis of the LeuP binding mode and the previous blLAP structures, different binding modes of the intermediate to the active site can be postulated. In the following discussion we will, starting from the possible binding modes of the tetrahedral transition state, evaluate their implication on the reaction pathway of peptide hydrolysis by LAP.

A new aspect of this inhibitor structure with respect to the intermediate binding mode is the possible coordination

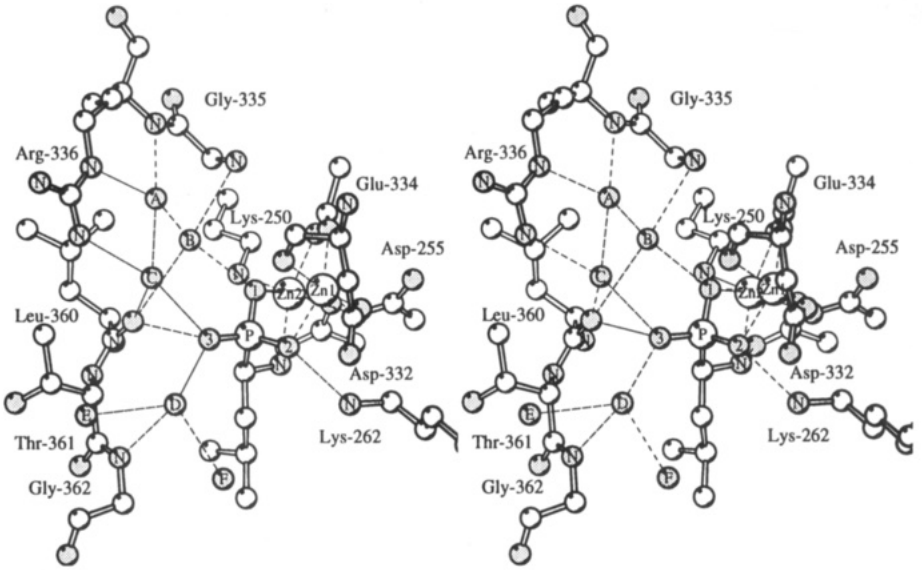

FIGURE 4: Active site structure of blLAP complexed with LeuP. The view is approximately from the central solvent cavity of the blLAP hexamer into the active site of one subunit. Besides the zinc ions, LeuP, and the labeled amino acids, the positions of five water molecules are shown. To facilitate the discussion, these water molecules have been labeled A−F. Metal coordination and hydrogen bonds are shown as thin, dashed lines.

FIGURE 5: Position of the site 3 metal-binding site relative to the dizinc active site. LeuP and the zinc ligands are shown as ball-and-stick models. Only Asp-273 coordinated to the dizinc center, Met-274, and the backbone carbonyl group of Asp-271 coordinated to the site 3 metal ion are labeled. The other ligands to the site 3 metal ion are the backbone carbonyl groups of Leu-170, Met-171, and Arg-271 at the carboxy end of the helix shown in the lower right corner of this figure.

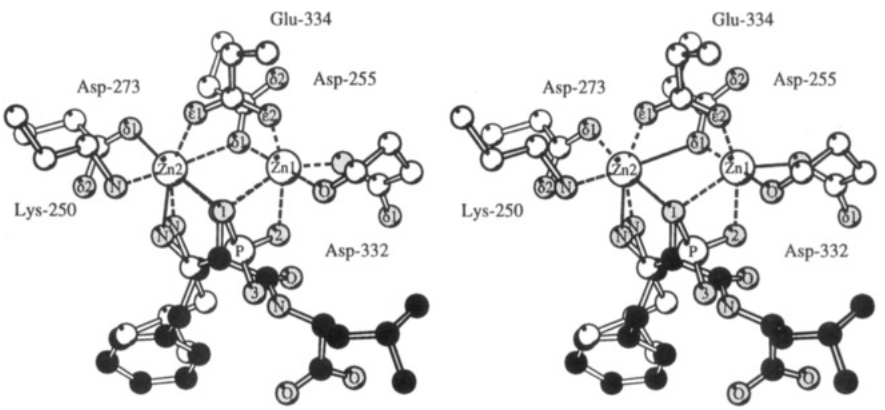

FIGURE 6: Superposition of bestatin and LeuP bound to the active site of blLAP. The atom positions of the zinc ions and the protein ligands are shown only for the blLAP−LeuP complex since the metal and protein ligand positions of both structures are very similar. Oxygen and nitrogen atoms are shown in gray. Carbon atoms of LeuP and the protein ligands are shown in white, and the carbon atoms of bestatin are shown in black.

of a third atom of the intermediate to the dizinc core, namely at the position of O2 of LeuP coordinated to Zn-488. In the bestatin and amastatin cocrystal structures, the P_1 carbonyl oxygen atom was next to the O2 position of the LeuP complex, but it did not coordinate to Zn-488, probably due to the considerable differences of these compounds from a peptide substrate. Another important result of the blLAP−LeuP inhibitor structure concerns the role of Arg-336 in catalysis. It was shown that for this inhibitor structure Arg-336 has no alternate conformations and does not directly

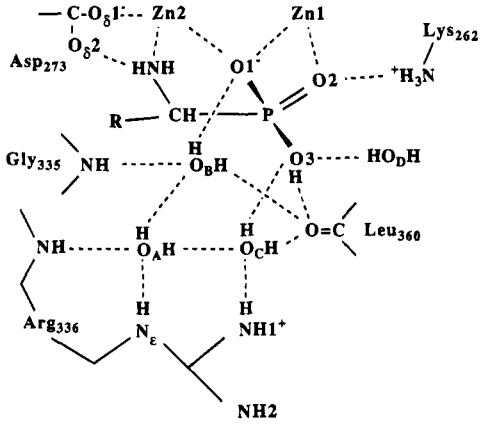

FIGURE 7: Proposed hydrogen-bonding pattern in the active site region. The hydrogen atoms were assigned to the noncarbon atoms on the basis of the hydrogen bond donor and acceptor capabilities of the residues and on the basis of the interatomic distances.

interact with the inhibitor. It seems now very likely that the V-shaped density in the previous inhibitor structures determined at a lower crystallographic resolution was caused by three adjacent water molecules and that Arg-336 does only interact with the substrate and the transition state via these water molecules.

On the basis of the amastatin and bestatin cocrystal structures and from steric considerations, it seems unlikely that in the transition state the position of the former peptide NH group corresponds to the bridging O1 position in the LeuP structure. Remaining are four possibilities for the binding of the transition state to the dizinc site, none of which can be *a priori* ruled out (Figures 8−10).

Mechanism I. This mechanism assumes that position O1 of the LeuP inhibitor complex corresponds to transition state atom O_n, the former attacking water nucleophile, O2 to O_c, and O3 to the NH group (Figures 8 and 10). The NH group of the peptide interacts with the main chain carbonyl group of Leu-360 upon substrate binding. Polarization of the peptide carbonyl group occurs by coordination to Zn1 and a hydrogen bond from Lys-262. A water molecule has been activated to the much stronger OH^- nucleophile by coordination to both zinc ions. The presence of a metal-bound water or hydroxide ion ligand remains to be shown for the native structure of blLAP. The previous structure determination at a crystallographic resolution of 2.32 Å in which the data were collected at ambient temperature did not allow an unambigous determination of one or more water molecules bound to the dizinc site (Burley et al., 1992). The tetrahedral intermediate is stabilized by the interaction of the negatively charged oxygen O_c with Zn-488 and Lys-262 as well as by the coordination of the hydroxyl group to both zinc ions. The NH group is hydrogen bonded to the carbonyl group of Lys-360 and to water molecule C, which protonates the amino group when the cleaved C-terminal part of the peptide substrate leaves the intermediate.

Mechanism II. This pathway differs from mechanism I in the positions and interactions of the carbonyl oxygen and the attacking nucleophile (Figures 8 and 10). The electrophilicity of the carbonyl carbon is enhanced by the coordination to both metal ions. The attacking nucleophile is a hydroxide ion, coordinated to Zn1 and stabilized by a hydrogen bond from Lys-262. The activation of the leaving group is identical to that in mechanism I. In the tetrahedral intermediate O_c is stabilized by the coordination to both metal ions and by a hydrogen bond from water B. O_n is coordinated to Zn-488 and hydrogen bonded to Lys-262.

Mechanism III. This mechanism is a modification of our previously proposed mechanism based on the bestatin and amastatin inhibitor structures (Burley et al., 1991; Kim & Lipscomb, 1993; 1994) (Figures 8 and 10). A new aspect of this mechanism in comparison with the previously proposed mechanism is the interaction of the former peptide nitrogen atom in the intermediate with Zn-488. The release of the leaving amino group is further promoted by the protonation of the NH group by Lys-262.

In the previously published formulation of this mechanism, Arg-336 interacted directly with the intermediate to stabilize the negative charge on atom O_c. It now seems likely that Arg-336 interacts with the substrate only via the three water molecules, A−C. The interaction of the presumably negatively charged oxygen O_c with water molecule C might appear only as a weak stabilization of the negatively charged oxygen atom compared to the stabilization by coordination to metal ions, as in carboxypeptidase A or thermolysin (Christianson & Lipscomb, 1989; Matthews, 1988), or by the positively charged guanidinium group of an arginine side chain. However, the tetrahedral intermediate of an associative acyl-transfer reaction can be stabilized by groups that can form hydrogen bonds to the negatively charged oxygen atom, as observed, for example, in the oxyanion hole of the serine proteinases. It has been proposed that short, strong hydrogen bonds might form if the pK_a of the donor group is similar to that of the neutral tetrahedral intermediate (Gerlt & Gassman, 1993), which is estimated to have a pK_a = 13.4 (Guthrie, 1974). The formation of strong hydrogen bonds might not only be feasible with peptidic NH groups ($pK_a \approx 15$; Bordwell, 1988), as proposed for a concerted general acid−general base mechanism for trypsin (Gerlt & Gassman, 1993), but also with protein-bound active site water molecules ($pK_a \approx 14$).

Mechanism IV. Mechanism IV assumes that in the transition state O_n corresponds to O3 in the LeuP structure and O_c to O1 (mechanism not shown as a figure). The interactions of the leaving group with Zn1 and Lys-262 are similar to those in mechanism III. This configuration would mean that the attacking water nucleophile comes from the region near Arg-336, where the three active site water molecules, A−C, are found in the LeuP−blLAP cocrystal structure. This possibility seems in comparison to mechanisms I−III much less likely since the water molecules in this region accept hydrogen bonds from the backbone NH group of Gly-335 and from Arg-336 (Figures 4 and 7), thus reducing the nucleophilicity of these water molecules. No adequate proton acceptor is present in this region that could activate a water molecule for nucleophilic attack in a general base type mechanism.

Comparison of the Possible Pathways. The superposition of the blLAP-LeuP structure with the blLAP−bestatin structure (Figure 6) showed that the P_1' peptide NH group of bestatin is nearest to the O3 oxygen atom of the LeuP inhibitor. It therefore seems reasonable to assume that the NH group of the substrate or intermediate will also bind there, thus favoring mechanisms I and II. Water molecules D and F (Figure 4) in the blLAP−LeuP structure are replaced upon substrate binding by the C-terminal fraction of the peptide substrate. There is no residue in position to accept

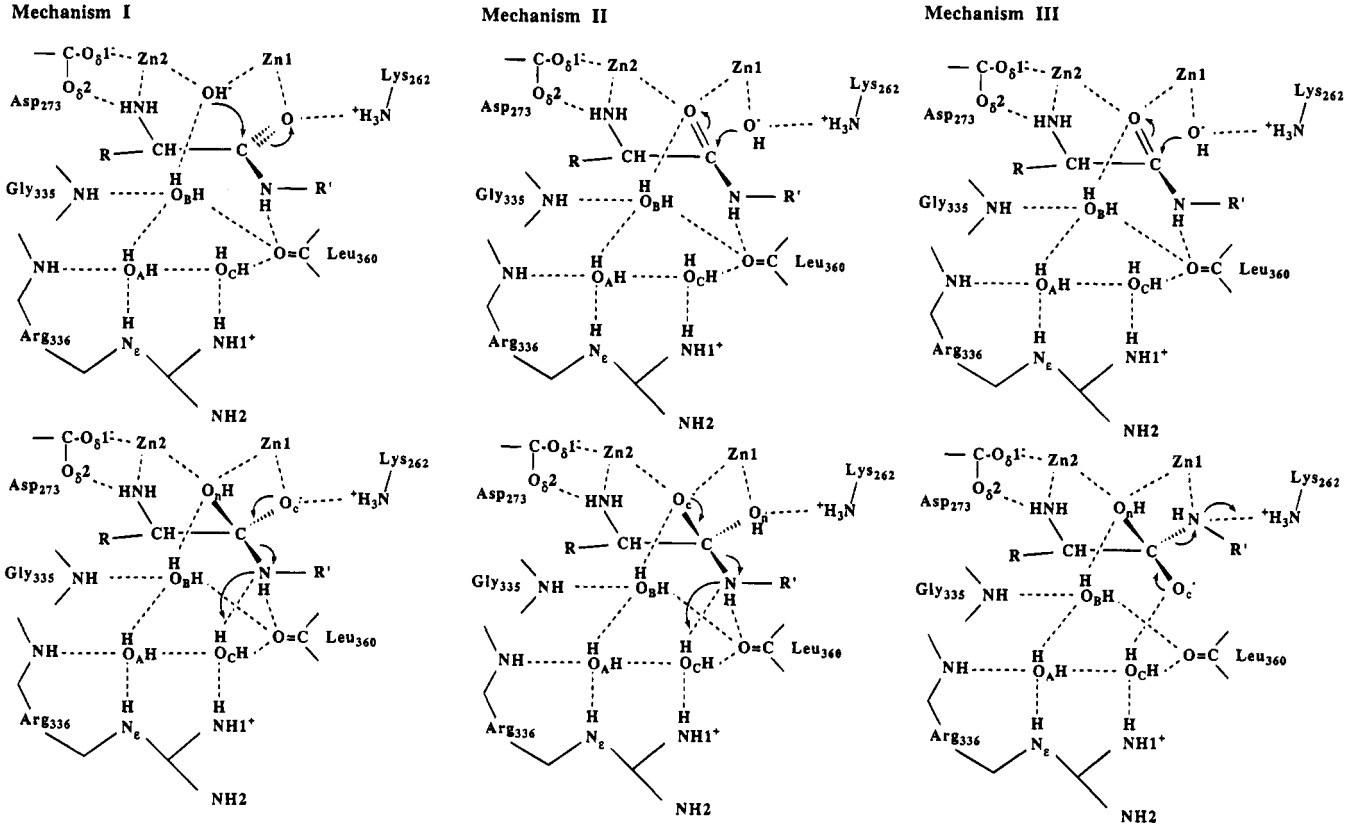

FIGURE 8: Three plausible mechanisms based on the blLAP−inhibitor structures determined so far. Mechanism I (left) assumes that position O1 in the blLAP−LeuP inhibitor is near the position of atom O_n, from the former attacking nucleophile (H_2O or OH^-) , in the tetrahedral intermediate. Furthermore, O2 corresponds to O_c and O3 to the P_1' NH group of the substrate. In mechanism II (middle) O1 corresponds to O_c, O2 to O_n, and O3 to NH. Mechanism III (right) assumes that O1 corresponds to O_n, O2 to NH, and O3 to O_c. Further details of the pathways are discussed in the text.

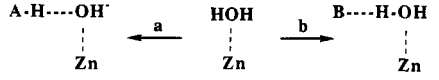

FIGURE 9: Scheme of general acid- and general base-assisted metal activation of a water nucleophile. By coordination to the metal ion, the pK_a of the water molecule is lowered. The water molecule may ionize and the resulting hydroxide ion be stabilized by a suitable hydrogen donor (general acid, a), or a general base may polarize the water molecule and accept the proton when the water molecule attacks the electrophilic center of the substrate (b).

a proton from the water nucleophile bound to the metal center, provided that the carboxylate groups coordinated to the zinc ions have a significantly lower pK_a value than the free carboxylic acid side chain groups, and therefore they are unlikely to act as a general base. In the absence of a general base that could assist the metals in generating an activated (polarized) water nucleophile, the coordination of the attacking water molecule to both metal ions as in mechanism I seems advantageous in order to generate a hydroxide ion nucleophile in comparison to the monodentate binding mode of the nucleophile. The presence of the protonated side chain of Lys-262 hydrogen bonded to the attacking OH^- as proposed in mechanism II (Figure 8) might seem unusual in comparison to a general base-assisted activation of the water nucleophile as found in several zinc enzymes, e.g., in carboxypeptidase A or thermolysin (Christianson & Lipscomb, 1989; Matthews, 1988). In a general acid-assisted activation of a water nucleophile, a metal-bound hydroxide ion is stabilized by hydrogen bonding to a general acid (Figure 9). In mechanism II Lys-262 is in a position to stabilize a zinc-bound hydroxide ion thus causing the Zn-OH_2/Zn-OH^- equilibrium to favor the stronger hydroxide ion nucleophile in a way which is similar to the effect of coordination to both metal ions.

The validity of all three possible mechanisms shown in Figure 8 has been examined by modeling the binding modes of the substrate L-leucyl-L-valine (LV) and the *gem*-diolate transition state LVTS for the three pathways (Figure 10). LV and LVTS have been modeled into the active site of blLAP in energetically favorable conformations under consideration of the inhibitor binding modes of bestatin, amastatin, and LeuP and under consideration of the binding interactions implied by the possible mechanisms. If an interaction of the nitrogen atom with Zn-488 is assumed, the transition state of mechanism III could be modeled only in an energetically unfavorable conformation of the dihedral angle along the scissile C−N bond. Alternatively, no stabilization of the leaving group by coordination to Zn-488 occurs, and the transition state can be modeled as shown previously (Kim & Lipscomb, 1993). A comparison of the stereochemistry of the possible pathways shows that in mechanism I the prochiral carbonyl group is attacked on the *re* enantiotopic face, whereas in mechanisms II and III the attack comes from the *si* side. The attacking nucleophile was modeled using a reasonable coordinating distance to the metal ion(s) (ca. 2−2.2 Å) and a distance of ca. 2.5 Å from the carbonyl carbon atom. Attack of the hydroxide ion on the carbon of the carbonyl group was modeled at approximately a 90° angle, although quantum chemical calculations showed that nucleophilic attack on the carbonyl group is not very sensitive to the attacking angle (Scheiner et al., 1976). In all three mechanisms water molecule C is in relatively close contact to the P_1' side chain of the peptide

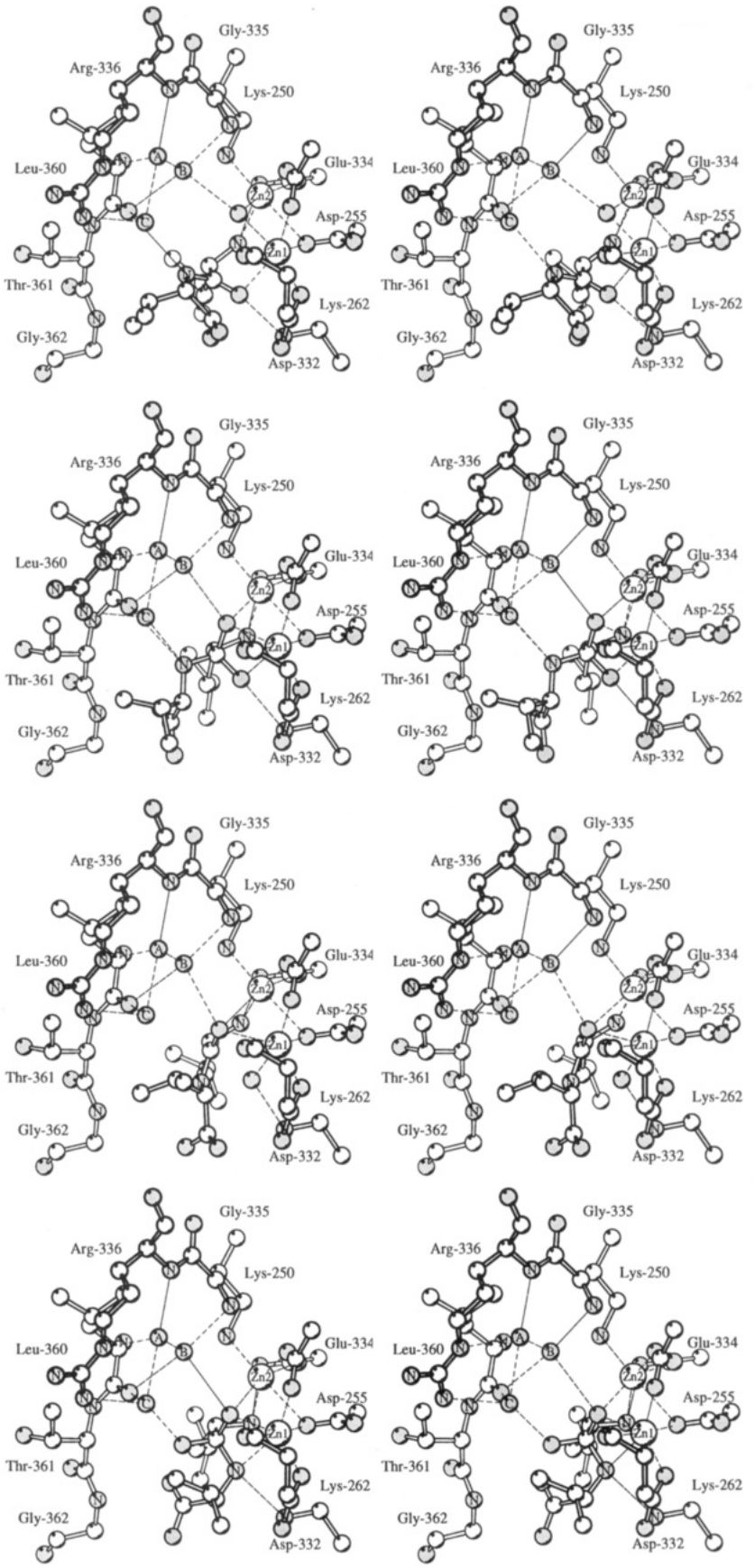

FIGURE 10: Substrate L-leucyl-L-valine (LV) and transition state (LVTS) binding modes modeled into the active site of blLAP according to mechanisms I−III on the basis of the binding modes of LeuP, bestatin, and amastatin. (Top) Proposed substrate binding mode for mechanism I. (Second from top) Intermediate binding modes for mechanisms I and II. For mechanism I the oxygen atom of the intermediate bridging both zinc ions is O_n, the former nucleophile, and the oxygen atom coordinated only to the site 1 zinc ion is O_c, the former carbonyl oxygen. For mechanism II the positions of these two oxygen atoms are exchanged. (Third from top) Substrate binding mode for mechanisms II and III. (Bottom) Intermediate binding mode of mechanism III including an interaction of the former peptide amino group with the site 1 zinc ion.

substrate. The *gem*-diolate intermediate is conformationally more flexible compared to the substrate, which has the planar carboxamide group, and the P_1' side chain is more distant from water molecule C. The three active site water molecules near Arg-336 may therefore occupy different positions when the substrate is bound as compared with those in the transition state structure. Since protein−bound water molecules visible in X-ray structures have very short residence times, ranging from below 500 ps to 0.01 s depending on the water environment (Levitt & Park, 1993), the change of a water position in a reaction pathway does usually not constitute a rate-limiting step.

All of the catalytic mechanisms discussed herein for blLAP assume that both metal ions have important roles in substrate binding as well as in catalysis with respect to the activation of the reactants. The mechanisms are thus in agreement with biochemical data showing that exchange of the zinc ions against other divalent metal ions in both binding sites influences k_{cat} as well as K_m (Allen et al., 1983). A special feature of the two-metal ion mechanism of LAP catalysis compared to the presumed pathways of catalysis of mononuclear zinc peptidases is the additional binding or stabilizing interactions between the metals and the reactants or the transition state: (1) the coordination of Zn-489 to the free N-terminus in order to bind and preorient the peptide substrate, (2) the activation of the attacking water as a nucleophile to a hydroxide ion ligand by coordination to both metal ions (mechanism I) or by a general acid-assisted formation of an OH^- nucleophile (mechanisms II and III), and (3) polarization of the carbonyl group by one or both metal ions. The role of Arg-336 has been redefined to interact with the substrate and intermediate via three water molecules. The protonated, positively charged guanidinium group of Arg-336 polarizes and lowers the pK_a of the water molecules A−C and enables them to form strong hydrogen bonds to the intermediate and/or to protonate the leaving group, as in mechanisms I and II. It remains to be shown whether a similar or different arrangement of the active site water molecules A−C is found in the structure of the native enzyme. A more detailed crystallographic analysis of the active site water structure of unligated blLAP may also reveal the presumed zinc-bound water or hydroxide ion ligand(s).

ACKNOWLEDGMENT

We gratefully acknowledge Prof. P. A. Bartlett for providing LeuP. We thank Dr. H. Kim for excellent discussions and reading of this manuscript and Dr. K. M. Reinisch for help in the cryocooling data collection.

REFERENCES

Allen, M. P., Yamada, A. H., & Carpenter, F. H. (1983) *Biochemistry 22*, 3778−3783.
Aoyagi, T., Tobe, H., Kojima, F., Hamada, M., Takeuchi, T., & Umezawa, H. (1978) *J. Antibiot. 31*, 636−638.
Bordwell, F. G. (1988) *Acc. Chem. Res. 21*, 456−463.
Brünger, A. T. (1992a) *X-PLOR Manual*, Version 3.1, Yale University, New Haven, CT.
Brünger, A. T. (1992b) *Nature 355*, 472−475.
Brünger, A. T., Krukowski, A., & Erickson, J. W. (1990) *Acta Crystallogr., Sect. A 46*, 585−593.
Burley, S. K., David, P. R., Taylor, A., & Lipscomb, W. N. (1990) *Proc. Natl. Acad. Sci. U.S.A. 87*, 6878−6882.
Burley, S. K., David, P. R., & Lipscomb, W. N. (1991) *Proc. Natl. Acad. Sci. U.S.A., 88*, 6916−6920.
Burley, S. K., David, P. R., Sweet, R. M., Taylor, A., & Lipscomb, W. N. (1992) *J. Mol. Biol. 224*, 113−140.
Carpenter, F. H., & Harrington, K. Y. (1972) *J. Biol. Chem. 247*, 5580−5586.
Carpenter, F. H., & Vahl, J. M. (1973) *J. Biol. Chem. 248*, 294−304.
Chakrabarti, P. (1990) *Protein Eng. 4*, 49−56.
Chevrier, B., Schalk, C., D'Orchymont, H., Rondeau, J., Moras, D., & Tarnus, C. (1994) *Structure 2*, 283−291.
Christianson, D. W., & Lipscomb, W. N. (1988) *J. Am. Chem. Soc. 110*, 5560−5565.
Christianson, D. W., & Lipscomb, W. N. (1989) *Acc. Chem. Res. 22*, 62−69.
Delange, R. J., & Smith, E. L. (1971) in *The Enzymes* (Boyer, P. D., Ed.) 3rd ed., Vol. III, pp 81−119, Academic Press, New York.
Fittkau, S., Förster, U., Pascual, C., & Schunck, W.-H. (1974) *Eur. J. Biochem. 44*, 523−528.
Gerlt, J. A., & Gassman, P. G. (1993) *Biochemistry 32*, 11943−11952.
Glusker, J. P. (1991) *Adv. Protein Chem. 42*, 1−76.
Giannousis, P. P., & Bartlett, P. A. (1987) *J. Med. Chem. 30*, 1603−1609.
Guthrie, J. P. (1974) *J. Am. Chem. Soc. 96*, 3608−3615.
Hanson, H., & Frohne, M. (1976) *Methods Enzymol. 45*, 504−521.
Harbeson, S. L., & Rich, D. H. (1988) *Biochemistry 27*, 7301−7310.
Jones, T. A., & Kjeldgaard, M. (1994) in *From First Map to Final Model. Proceedings of the CCP4 Study Weekend* (Bailey, S., Hubbard, R., & Waller, D., Eds.) pp 1−13, Daresbury Laboratory, Warrington, U.K.
Jurnak, F., Rich, A., van Loon-Klaassen, L., Bloemendal, H., Taylor, A., & Carpenter, F. (1977) *J. Mol. Biol. 112*, 149−153.
Kabsch, W. (1988) *J. Appl. Crystallogr. 21*, 67−71.
Kaplan, A. P., & Bartlett, P. A. (1991) *Biochemistry 30*, 8165−8170.
Kim, H., & Lipscomb, W. N. (1991) *Biochemistry 30*, 8171−8180.
Kim, H., & Lipscomb, W. N. (1993a) *Biochemistry 32*, 8465−8478.
Kim, H., & Lipscomb, W. N. (1993b) *Proc. Natl. Acad. Sci. U.S.A. 90*, 5006−5010.
Kim, H., & Lipscomb, W. N. (1994) *Adv. Enzymol. 68*, 153−213.
Kraulis, P. (1991) *J. Appl. Crystallogr. 24*, 946−950.
Levitt, M., & Park, B. (1993) *Structure 1*, 223−226.
Luzzati, P. V. (1952) *Acta Crystallogr. 5*, 802−810.
Matthews, B. W. (1988) *Acc. Chem. Res. 21*, 333−340.
Melbye, S. W., & Carpenter, F. H. (1971) *J. Biol. Chem. 246*, 2459−2463.
Molecular Simulations Inc. (1994) QUANTA, V. 4. O. , Burlington, MA.
Navaza, J. (1994) *Acta Crystallogr., Sect. A 50*, 157−163.
Rich, D. H., Moon, B. J., & Harbeson, S. (1984) *J. Med.Chem. 27*, 417−422.
Roderick, S. L., & Matthews, B. W. (1993) *Biochemistry 32*, 3907−3912.
Schechter, I., & Berger, A. (1967) *Biochem. Biophys. Res. Commun. 27*, 157−162.
Scheiner, S., Lipscomb, W. N., & Kleier, D. A. (1976) *J. Am. Chem. Soc. 98*, 4770−4777.
Smith, E. L., & Hill, R. L. (1960) in *The Enzymes* (Boyer, P. D., Lardy, H., & Myrback, K., Eds.) 2nd ed., Vol. 4, Part A, pp 37−63, Academic Press, New York.
Taylor, A. (1993a) *TIBS 18*, 167−172.
Taylor, A. (1993b) *FASEB J. 7*, 290−298.
Taylor, A., Daims, M. A., Lee, J., & Surgenor, T. (1982) *Curr. Eye. Res. 2*, 47−56.
Taylor, A., Peltier, C. Z., Torre, F. J., & Hakamian. (1993) *Biochemistry 32*, 784−790.
Thompson, G. A., & Carpenter, F. H. (1976a) *J. Biol. Chem. 251*, 53−60.
Thompson, G. A., & Carpenter, F. H. (1976b) *J. Biol. Chem. 251*, 1618−1624.
Umezawa, H., Ishizuka, M., Aoyagi, T., & Takeuchi, T. (1976) *J. Antibiot. 29*, 857−859.
Umezawa, H. (1980) *Recent Results Cancer Res. 75*, 115−125.

BI950928H